

Contents lists available at [ScienceDirect](#)

Journal of Sound and Vibration

journal homepage: www.elsevier.com/locate/jsvi

Collocation approach to the Helmholtz eigenvalue problem on multiply connected domains

Paolo Amore^{a,*}, Diego Chowell^b^a *Facultad de Ciencias, CUICBAS, Universidad de Colima, Bernal Díaz del Castillo 340, Colima, Colima, Mexico*^b *Facultad de Ciencias, Universidad de Colima, Bernal Díaz del Castillo 340, Colima, Colima, Mexico*

ARTICLE INFO

Article history:

Received 14 July 2009

Received in revised form

1 September 2009

Accepted 9 November 2009

Handling Editor: M.P. Cartmell

ABSTRACT

We present a collocation approach to the numerical solution of the Helmholtz eigenvalue problem on multiply connected domains of arbitrary shape in two dimensions. A suitable representation of the Helmholtz equation on a uniform grid is obtained and the problem is converted to the calculation of the first few eigenvalues and eigenvectors of a large sparse matrix. The accuracy of this approach is tested by performing a comparison with results available in the literature. The flexibility and simplicity of the method make easy the application to arbitrary geometries.

© 2009 Elsevier Ltd. All rights reserved.

1. Introduction

In this paper we use a collocation method to obtain numerical solutions to the Helmholtz equation on multiply connected domains in the plane. This problem has been considered recently in [1,2,4–6], using different approaches. In particular, Wang has studied the vibration of polygonal membranes with a central circular hole, varying the size of the hole: for holes of vanishing radius he has derived an asymptotic formula for the frequency, showing that the frequency for an annular membrane pinned at the origin is unaffected; for holes of finite size he has used a point matching method, considering membranes of square, hexagonal and octagonal shape. More recently Chen and collaborators have used the boundary element method (BEM), which is known to provide spurious solutions when applied to multiply connected domains. The elimination of these spurious modes, however, is possible and it has been discussed for example in [2], where the reader may also find an extensive discussion on the literature relevant for this subject. Finally Reutskiy [6] has also formulated a new boundary element method for the Helmholtz problem on simply and multiply connected domains: this method does not involve the evaluation of a determinant and allows to reach precise results.

In this paper the same problem is studied using a collocation approach, already applied in [7,8] to solve the Helmholtz equation in simply connected domains of the plane, both for homogeneous and inhomogeneous membranes. Despite the flexibility and simplicity of the present approach, we will show that it yields precise results and we will compare our findings with specific examples taken from the literature. The paper is organized as follows: in Section 2 we outline our method and introduce the set of functions which are used for the collocation; in Section 3 we report the numerical results obtained with our method and compare them with analogous results from the literature; finally, in Section 4 we state the main conclusions of this paper.

* Corresponding author.

E-mail address: paolo.amore@gmail.com (P. Amore).

2. The method

The method that we use in this paper to obtain numerical solutions to the Helmholtz equation on multiply connected regions is based on a collocation approach, which allows the discretization of a finite two-dimensional region of the plane using a set of function, called *Little Sinc functions* (LSF) (see [7–10]). These functions were originally obtained in [11], where they were called “first sine basis”. Previous applications of these functions include the Schrödinger equation in one dimension, within a variational approach [9], the representation of non-local operators on a uniform grid, which has been applied to the solution of the relativistic Salpeter equation [10], the Helmholtz equation on arbitrary two-dimensional domains both for the homogeneous [7] and the inhomogeneous [8] case. In particular the last two references are the most relevant for the discussion carried out here. LSF corresponding to different boundary conditions have been recently derived in [12].

To make our discussion self-contained we briefly review the main features of our approach, starting with the set of functions which are used for the discretization. A Little Sinc function (LSF) is obtained as an approximate representation of the Dirac delta function in terms of the wave functions of a particle in a box (being $2L$ the size of the box):

$$s_k(h, N, x) \equiv \frac{1}{2N} \left\{ \frac{\sin((2N+1)\chi_-(x))}{\sin\chi_-(x)} - \frac{\cos((2N+1)\chi_+(x))}{\cos\chi_+(x)} \right\}, \tag{1}$$

where $\chi_{\pm}(x) \equiv (\pi/2Nh)(x \pm kh)$. The index k takes the integer values between $-N/2+1$ and $N/2-1$ (N being an even integer). The LSF corresponding to a specific value of k is peaked at $x_k = 2Lk/N = kh$, h being the grid spacing and $2L$ the total extension of the interval where the function is defined. Moreover the functions belonging to this set obey the useful property $s_k(h, N, x_j) = \delta_{kj}$. These properties are clearly evident in Fig. 1, where three different LSF corresponding to $N = 10$ and $L = 1$ are plotted.

Different functions belonging to the same set are also found to be orthogonal

$$\int_{-L}^L s_k(h, N, x)s_j(h, N, x) dx = h\delta_{kj}. \tag{2}$$

Using the properties above one can approximate a function defined on $x \in (-L, L)$ as

$$f(x) \approx \sum_{k=-N/2+1}^{N/2-1} f(x_k)s_k(h, N, x). \tag{3}$$

In a similar fashion one can also obtain a representation of the derivative of a LSF within the same set of LSF as

$$\begin{aligned} \frac{ds_k(h, N, x)}{dx} &\approx \sum_j \left. \frac{ds_k(h, N, x)}{dx} \right|_{x=x_j} s_j(h, N, x) \equiv \sum_j c_{kj}^{(1)} s_j(h, N, x), \\ \frac{d^2s_k(h, N, x)}{dx^2} &\approx \sum_j \left. \frac{d^2s_k(h, N, x)}{dx^2} \right|_{x=x_j} s_j(h, N, x) \equiv \sum_j c_{kj}^{(2)} s_j(h, N, x), \end{aligned} \tag{4}$$

where the analytical expressions for the coefficients $c_{kj}^{(r)}$ can be found in [9]. Clearly Eq. (3) is approximate, however, the error made with this approximation is bound to decrease with N , as discussed in Ref. [9]. The effect of this approximation is to discretize the continuum of an interval of size $2L$ on the real line into a discrete set of $N - 1$ points, x_k , uniformly spaced

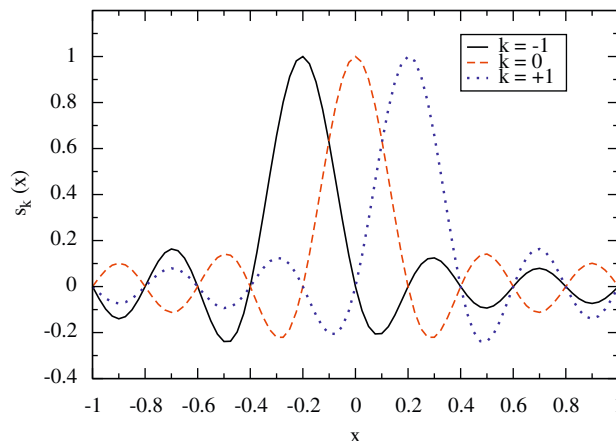


Fig. 1. Three LSF for $N = 10, L = 1$ corresponding to $k = -1, 0, +1$.

on this interval. In particular, we may consider the one-dimensional Helmholtz equation

$$-\frac{d}{dx^2}\psi_n(x) = k_n^2\psi_n(x), \tag{5}$$

with $\psi_n(\pm 1) = 0$. Using Eq. (4) we obtain a matrix representation for the second derivative operator on the grid, whose matrix elements are analytically known and correspond to the $c_{kj}^{(2)}$ in Eq. (4). In the following we will use the notation

$$\hat{H}^{(d)} \equiv -\left(\frac{\partial^2}{\partial x_1^2} + \dots + \frac{\partial^2}{\partial x_d^2}\right) = -\Delta_d$$

to indicate the negative Laplacian operator in d dimensions; our result in one-dimensional may therefore be written as

$$H_{kj}^{(1)} = c_{kj}^{(2)}. \tag{6}$$

Notice that since the indices k, j span $N - 1$ values, a $(N - 1) \times (N - 1)$ matrix, $H^{(1)}$, is obtained: its eigenvalues and eigenvectors are approximations to the frequencies and wave functions of the equation in the continuum. Actually in the case of Eq. (5) the matrix corresponding to the discretized second derivative provides the *exact solutions*, since the LSF itself are built using the solutions of Eq. (5) (see Ref. [9]).

We may now extend the discussion to two dimensions: on a plane, one may generate a set of functions obtained by the direct product of the $N_x - 1$ and $N_y - 1$ LSF in the x - and y -axis: this operation generates a uniform rectangular grid with spacings h_x and h_y (in the following we will limit ourselves to square grids). Although a point on this grid is clearly identified by a pair of integers numbers, (k, k') , one prefers to be able to use a single integer to specify the location of the point:

$$K \equiv k' + \frac{N}{2} + (N - 1)\left(k + \frac{N}{2} - 1\right), \tag{7}$$

which takes the values $1 \leq K \leq (N - 1)^2$, $(N - 1)^2$ being the total number of points on the grid. This relation can also be inverted

$$k = 1 - N/2 + \left\lceil \frac{K}{N - 1 + \varepsilon} \right\rceil, \tag{8}$$

$$k' = K - N/2 - (N - 1)\left\lceil \frac{K}{N - 1 + \varepsilon} \right\rceil, \tag{9}$$

where $[a]$ is the integer part of a real number a and $\varepsilon \rightarrow 0$.

In the case at hand we are interested in the solution of the Helmholtz equation on a two-dimensional square region Ω , i.e. we wish to solve the equation

$$-\nabla^2\psi_n(x, y) = k_n^2\psi_n(x, y), \tag{10}$$

where $(x, y) \in \Omega$, supplemented by Dirichlet bc on $\partial\Omega$. The discretization of this equation using the set of functions obtained above is straightforward and leads to

$$H_{kj, k'j'}^{(2)} = -[c_{kj}^{(2)}\delta_{k'j'} + \delta_{kj}c_{k'j'}^{(2)}], \tag{11}$$

where $(k, j, k', j') = -N/2 + 1, \dots, N/2 - 1$. At this point we wish to make few remarks on this equation: first, we notice that (11) is analytical, second, that it has a tensorial nature since it connects two points on the grid; it is straightforward to obtain a matricial representation using Eq. (7). We thus obtain a $(N - 1)^2 \times (N - 1)^2$ square matrix, whose elements are given by Eq. (11).

Although the approach described so far is specific to a rectangular region of the plane, which is the natural support of the LSF, we may generalize it to arbitrary regions using two different approaches, both of which have been discussed in [7]. The more precise approach is based on the conformal map of the arbitrary region onto a square: in this case the homogeneous Helmholtz equation on the original region is mapped to an inhomogeneous Helmholtz equation on the square, where the density is obtained directly for the derivative of the conformal map (see [13]). The numerical results obtained in [7] for a circular membrane and for a circular waveguide indicate that the convergence toward the exact result is proportional to h^4 , h being the grid spacing. The drawback of this approach is the cost of obtaining a conformal map, either analytically, when possible, or numerically, for arbitrary regions of the plane.

The second approach to this problem is based on the observation that a given LSF is *peaked* on a specific grid point and that if this function is removed from the set then any function obtained from the linear combination of the remaining elements of the set will necessarily vanish on this grid point (remember the property $s_k(h, N, x_j) = \delta_{kj}$). It is therefore possible to implement approximate Dirichlet bc on the border of the region by rejecting all grid points which are external to the membrane. This procedure is illustrated in Fig. 2, where we have plotted a square membrane of size $\ell = 2$, with a central circular hole of radius $R = \frac{1}{2}$. In this case we use a square grid of 361 points ($N = 20$), although the matrix obtained with the collocation procedure is just of dimensions 280×280 . Notice that the internal circular border is not sampled exactly from the grid, and the ratio between the number of allowed points to the total points is bound to fluctuate as grid

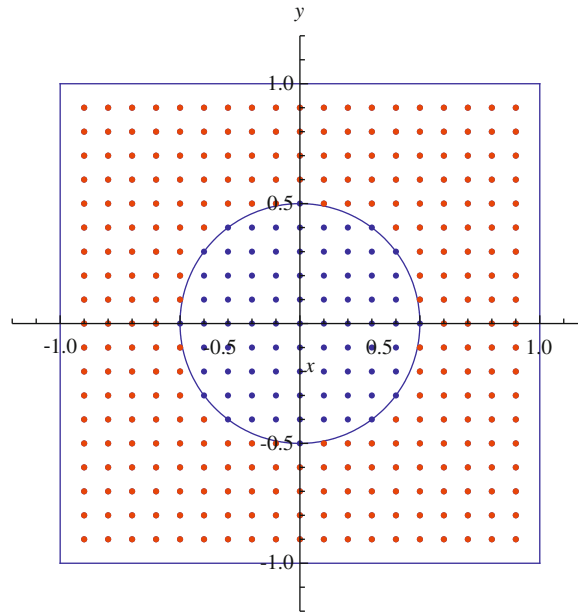


Fig. 2. Square membrane with a circular hole. The points are the collocation points corresponding to $N = 20$: the dots external (internal) to the circle are kept (rejected).

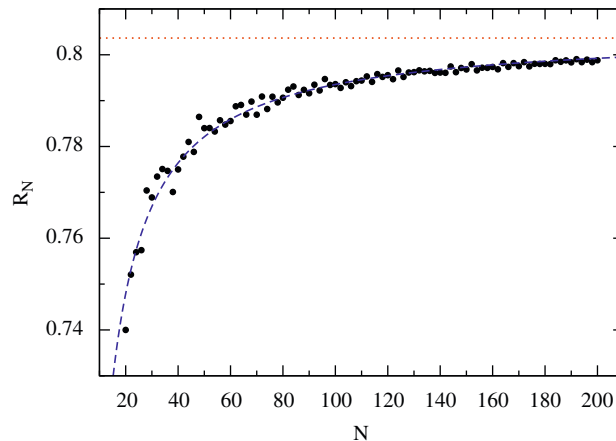


Fig. 3. Ratio of allowed to total points of the grid for a square membrane with a circular hole. The horizontal line is the geometric ratio, while the dashed line is the fit $R_N^{\text{fit}} = 0.805 - 1.14/N$.

size decreases. The amplitude of the fluctuations also decreases with larger N . The behavior for this particular membrane is illustrated in Fig. 3, where we have plotted the ratio R_N between the number of grid points belonging to the membrane and the total number of grid points, as a function of N . In the limit $N \rightarrow \infty$, R_N tends to the geometric ratio $\mathcal{R} = 1 - \pi/16 \approx 0.804$, the horizontal line in the figure. The dashed line is the fit $R_N^{\text{fit}} = 0.805 - 1.14/N$, which suggests that the convergence toward the exact result will now be of order h (remember that $h = 2L/N$). Notice that the fit approximates \mathcal{R} with an error of just 0.2 percent. An important aspect to stress is that, although R_N gives important information on the expected accuracy of the approximation at a given N , it does not involve the previous calculation of eigenvalues/eigenvectors and therefore it has a limited computational cost. By using the information contained in R_N we may be able to select more convenient grids, before having to calculate the eigenvalues. The second aspect that should be clear from this discussion is that following the procedure that we have illustrated one is able to treat approximately the Helmholtz equation on multiply connected domains of arbitrary shape, with an arbitrary number of holes. An assessment of the accuracy that can be achieved using this method will be made in the next section, performing a comparison with results available in the literature.

We like to point out that the matrices obtained with this collocation procedure are sparse. Efficient iterative methods to obtain selected eigenvalues or eigenvectors of a large sparse matrix are available: the main limitation of these methods is

not the dimension of the matrix itself, but rather the number of non-zero elements of the matrix, which determines the amount of memory effectively needed on a computer. For example, in the case of Fig. 2, the number of non-zero elements is $N^{nz} = 8696$, over a total of $N^{tot} = 78\,400$ elements. Luckily enough, the sparseness of the matrices is also increasing as the grid becomes finer (for example, for a grid corresponding to $N = 50$, $N^{nz} = 158\,232$ and $N^{tot} = 3\,655\,744$). While for grids with moderate number of points we have used the built-in Mathematica commands to obtain the eigenvalues and eigenvectors of the matrices, for the finest grids considered in this paper we have used the *conjugate gradient method* (CGM), which typically converges quite rapidly and requires less memory.

We wish to conclude this section sketching the extension of the present approach to three-dimensional problems (with or without holes). In three dimensions the LSF define a cubic grid with $(N - 1)^3$ internal points. Clearly a point on this grid is identified by a triplet of integers (k, k', k'') and thus the discretization of the Helmholtz equation on this grid leads to an expression which depends on six indices:

$$H_{kk'k''jjj''}^{(3)} = - [c_{kj}^{(2)} \delta_{k'j'} \delta_{k''j''} + c_{k'j'}^{(2)} \delta_{kj} \delta_{k''j''} + c_{k''j''}^{(2)} \delta_{kj} \delta_{k'j'}]. \tag{12}$$

In order to obtain a matrix representation of \hat{H} on the grid, one needs to generalize Eqs. (7)–(9). The generalized relations read

$$K = k'' + \frac{N}{2} + (N - 1) \left(k' + \frac{N}{2} - 1 \right) + (N - 1)^2 \left(k + \frac{N}{2} - 1 \right) \tag{13}$$

and

$$k = 1 - \frac{N}{2} + \left[\frac{K}{(N - 1)^2 + \varepsilon} \right], \tag{14}$$

$$k' = 1 - \frac{N}{2} + \left[\frac{K - (N - 1)^2 (k + N/2 - 1)}{(N - 1) + \varepsilon} \right], \tag{15}$$

$$k'' = K - N/2 - (N - 1)^2 \left(k + \frac{N}{2} - 1 \right) - (N - 1) \left(k' + \frac{N}{2} - 1 \right). \tag{16}$$

In this way a point on the grid may be identified with a single integer K which takes the values from 1 to $(N - 1)^3$ and Eq. (12) provides the elements of a $(N - 1)^3 \times (N - 1)^3$ matrix. The reader will notice that the only difference with respect to the two-dimensional case discussed above stays in the dimensionality of the matrix, which in d dimensions would be $(N - 1)^d \times (N - 1)^d$. The amount of memory available to store this (sparse) matrix is the only limitation to the application of the present approach to higher dimensional problems. Concerning the solution of the Helmholtz equation in d dimensions for regions of arbitrary shapes (with or without holes), the same considerations made earlier hold: only the points of the grid internal to the volume are kept and used to obtain a matrix representing the Laplacian on the grid. The few lower eigenvalues and eigenvectors of this matrix may be obtained again using the same procedures followed in two dimensions.

Finally we point out that the approach described in this paper does not suffer the presence of spurious modes, which is common to other approaches: while the empirical evidence of this claim can be obtained from the examples considered in the next section, we may also provide a qualitative justification. Strictly speaking, the LSF corresponding to a finite grid do not form a basis: as a matter of fact the LSF functions obtained for a fixed N are built using the N lowest eigenfunctions of a particle in a box, as shown in [9]. Therefore we may argue that LSF with N fixed span a subspace of the whole Hilbert space of solutions. The general solution to the Helmholtz equation may be obtained as a linear combination of the elements of the basis: in particular, for a solution corresponding to lower energy (frequency) the states in the Hilbert space with lowest energy will provide larger contributions. This statement may be rephrased in terms of the LSF as the possibility of accurately interpolating functions with a wavelength $\lambda \gg h$, where h is the grid spacing $h = 2L/N$. With this simple argument we expect that the lowest part of the spectrum of the matrix representing the negative Laplacian on the uniform grid will reproduce the corresponding low energy physical spectrum, up to wavelengths where the constraint given above holds.

The reader may find useful the flowchart in Fig. 4 which illustrates our method.

3. Numerical results

3.1. Example 1: annular membrane

The first example that we wish to consider is an annular membrane with radiuses $r^{max} = 2$ and $r^{min} = \frac{1}{2}$. Our results are reported in Table 1 where they are compared with the results reported in Ref. [2], using the *finite element method* (FEM) and the *boundary element method* (BEM), and with the exact results, which can be easily calculated in this example.

It is interesting to notice that, even with a limited number of grid points (LSF₅₀), the collocation approach provides results which are very close to those of BEM and FEM: in particular our results approximate better the exact results than the FEM results.

In Table 2 we report the results for the membrane obtained by shifting the center of the circular hole of the previous membrane at the point (0.5, 0). This example is discussed in [2,6]. Notice that the results of [6], while possibly being the most precise, fail to identify exactly the upper three eigenvalues, which are marked in the table with † (evidently the two last pair of modes, the seventh and the eighth mode on one side, and the ninth and the tenth on the other, which are almost

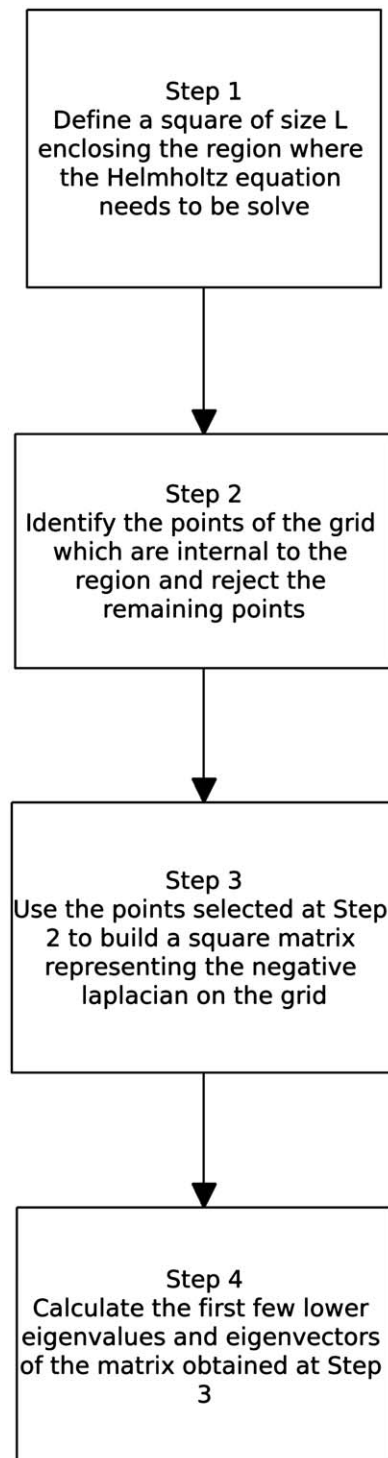


Fig. 4. Flowchart illustrating the method.

Table 1

First 10 eigenvalues of the Helmholtz equation on an annular domain.

	1	2	3	4	5	6	7	8	9	10
LSF ₅₀	2.00	2.18	2.18	2.62	2.63	3.19	3.19	3.77	3.78	4.06
LSF ₁₀₀	2.02	2.20	2.20	2.64	2.64	3.20	3.20	3.78	3.78	4.11
FEM of Ref. [2]	2.03	2.20	2.20	2.62	2.62	3.15	3.15	3.71	3.71	4.06
BEM of Ref. [2]	2.06	2.23	2.23	2.67	2.67	3.22	3.22	3.81	3.81	4.18
Exact	2.0489	2.2238	2.2238	2.6600	2.6600	3.2132	3.2132	3.7992	3.7992	4.1619

Table 2

First 10 eigenvalues of the Helmholtz equation on an annular domain with the interior hole shifted.

	1	2	3	4	5	6	7	8	9	10
LSF ₅₀	1.71	2.11	2.44	2.74	2.92	3.29	3.32	3.33	3.81	3.83
LSF ₁₀₀	1.72	2.12	2.44	2.75	2.93	3.30	3.33	3.35	3.83	3.84
FEM of Ref. [2]	1.73	2.13	2.45	2.76	2.95	3.30	3.34	3.36	3.83	3.84
Ref. [3]	1.75	2.14	2.47	2.78	2.97	3.33	3.37	3.38	3.85	3.87
Ref. [6]	1.74	2.13	2.46	2.77	2.96	3.31	3.38	3.86 [†]	4.28 [†]	4.41 [†]

Table 3

First 10 eigenvalues of the Helmholtz equation on a circular domain with a central square hole.

	1	2	3	4	5	6	7	8	9	10
LSF ₅₀	2.15	2.30	2.30	2.66	2.74	3.22	3.22	3.78	3.78	4.34
LSF ₁₀₀	2.15	2.30	2.30	2.66	2.74	3.22	3.22	3.79	3.79	4.33
FEM of Ref. [2]	2.19	2.33	2.33	2.67	2.76	3.22	3.22	3.76	3.77	4.32
BEM of Ref. [2]	2.19	2.33	2.33	2.69	2.76	3.24	3.24	3.81	3.81	4.40

Table 4

First 10 eigenvalues of the Helmholtz equation on a circular domain with an eccentric square hole.

	1	2	3	4	5	6	7	8	9	10
LSF ₅₀	1.80	2.20	2.50	2.79	3.05	3.38	3.38	3.47	3.84	3.90
LSF ₁₀₀	1.80	2.20	2.50	2.80	3.08	3.40	3.45	3.47	3.87	3.93
FEM of Ref. [2]	1.81	2.20	2.50	2.79	3.07	3.36	3.40	3.41	3.79	3.85
BEM of Ref. [2]	1.81	2.21	2.53	2.83	3.10	3.42	3.47	3.47	3.90	3.95

degenerate, appear only once in Reutsky results). A clear advantage of the collocation approach is that it provides the correct sequence of eigenvalues and that spurious results are not present.

3.2. Example 2: circular membrane with a square hole

In Table 3 we consider a circular membrane with a central square hole. The circle has radius $R=2$ and the square has side $\ell=1$. A comparison is made with the results of [2] (last two rows).

In Table 4 we consider the membrane of the previous example, where the square hole has now been centered around $(0.5, 0)$. The last two rows are the results taken from [2].

3.3. Example 3: polygonal membranes with a central circular hole

In Table 5 we have considered the examples of a square, hexagonal and octagonal membrane with a central circular hole. These examples were considered in Wang 1998 and later studied also in [4]. The last four rows are the results taken from these references.

In Fig. 5 we plot the frequency of the fundamental mode of the hexagonal membrane with a central circular hole obtained by using our collocation approach in two slightly different ways. This problem has been discussed in [1,4]. The circles in the plot represent the results obtained by discretizing the problem, with the hexagon oriented to have two sides parallel to the x -axis; the squares in the plot represent the results obtained by performing a scale transformation on the original problem which moves these faces of the hexagon to coincide with the sides of the square where the LSF are

Table 5

Fundamental eigenvalues of polygonal cavities with inner circular hole.

	Square	Hexagonal	Octagonal
LSF ₅₀	5.00	5.55	5.75
LSF ₁₀₀	5.06	5.62	5.90
Ref. [1]	5.09	5.76	5.97
BEM of Ref. [4]	5.07	5.74	5.94
CHIEF of Ref. [4]	5.08	5.75	5.96
Null-field of Ref. [4]	5.08	5.74	5.93

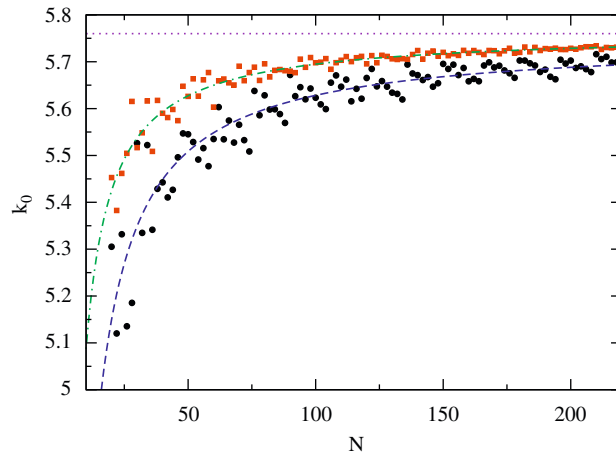


Fig. 5. Frequency of the fundamental mode of a hexagonal membrane with a central circular hole: the circles are obtained by orienting the membrane to have two sides parallel to the x -axis; the squares are the results obtained by performing a scale transformation in the y direction to make these two sides fall on the border of the square. The horizontal line is the result of [1], whereas the two dashed curves are fits of the two sets of data.

defined. Notice that this operation also changes the shape of the hole, which now becomes elliptical, and the form of the Laplacian operator. The horizontal line is the precise result of [1], whereas the dashed line corresponds to the fits of the two set of data, respectively, $k_0^{fit} = 5.75 - 11.97/N$ and $k_0^{fit} = 5.76 - 6.75/N$. The most striking feature of the first set of data is the oscillating behavior, which is much milder in the case of the second set of data. This behavior is due to the two horizontal sides of the hexagon, which are not sampled precisely, since the grid does not pass through them: consequently, as N is increased, for particular values of N a whole set of points may move from one side of the border to the other, causing a sudden rise or drop in the value of the eigenvalue. This effect, while maximal for horizontal or vertical lines, is much weaker for arbitrary lines, where some points may migrate in one direction and other points in the opposite direction, thus leading to smaller oscillations.

In Fig. 6 we have plotted the ratio between the collocation points internal to the membrane and the total number of grid points (the solid circles) and compared with the frequency of the fundamental mode (the solid squares), which has been shifted to allow better comparison. As previously mentioned, the calculation of R_N involves a limited computational effort, however, it carries interesting informations on the spectrum, as it can be seen from the figure. In particular we observe that, as expected, the eigenvalues are minimal at the values of N where the ratio is maximal.

3.4. Example 4: circular membrane with four circular holes

Another example which we have studied is a circular membrane of radius $R = 1$ with four circular holes of radius $r = 0.1$ at a distance $d = 0.5$ from the origin as shown in Fig. 7. This problem has been studied in [14], where the first five frequencies have been calculated. We have used our collocation approach to obtain numerical solutions for the even–even states of this membrane: by using the symmetry of the problem one is able to reduce by 4 the size of the collocation matrices. We have obtained two sets of results: one using the configuration shown in the figure and one using the configuration obtained by rotating the membrane of an angle $\pi/4$. In Table 6 we report the numerical results for the first three frequencies: the first three columns are the numerical results obtained with $N = 50, 100$ and fitting the results from $N = 20$ to 220 for the configuration of Fig. 7; the remaining three columns are the similar results for the configuration rotated by $\pi/4$. It is interesting to see that k_2 is different for the two configurations: although one could suspect a numerical error, this result is actually correct since the second even–even mode in the rotated configuration is odd–odd when seen in the original configuration and therefore absent from the first column. The results obtained with a fit (third and sixth column) are remarkably close to those of [14].

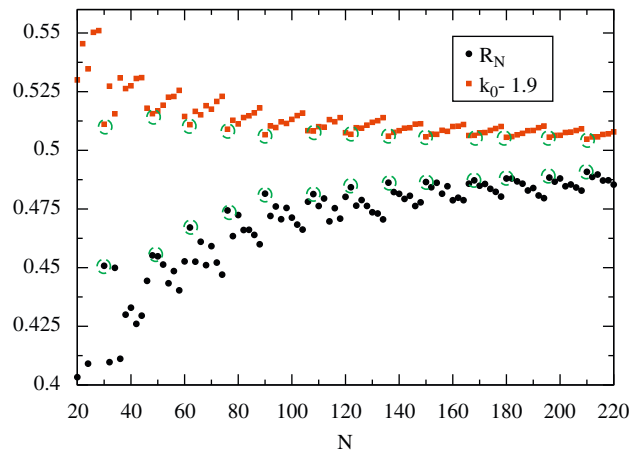


Fig. 6. Geometric ratio R_N and fundamental frequency of the hexagonal membrane with a central circular core and two sides parallel to the x -axis. The circles are the ratio between the collocation points internal to the membrane and the total number of grid points; the squares represent the frequency of the fundamental mode, which has been shifted to allow better comparison. The dashed circles in the plot identify the specific values of N where the ratio is minimal and the eigenvalues are maximal.

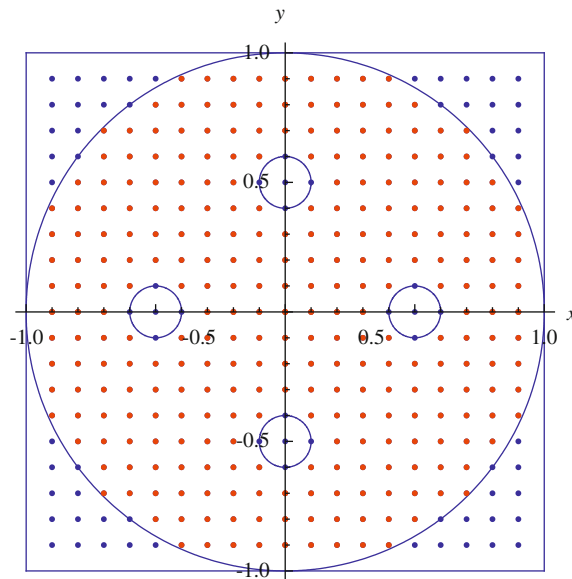


Fig. 7. Circular membrane of radius $R = 1$ with four circular holes of radius $r = 0.1$. The points in the figure correspond to a grid with $N = 20$.

Table 6

First three even-even frequencies of the Helmholtz equation on a circular domain with four circular holes.

	LSF_{50}	LSF_{100}	LSF_{FIT}	LSF_{50}^*	LSF_{100}^*	LSF_{FIT}^*
k_1	4.45	4.46	4.48	4.28	4.44	4.50
k_2	5.88	5.91	5.94	5.44	5.50	5.54
k_3	7.16	7.19	7.25	5.87	5.90	5.95

3.5. Example 5: square membrane with a rotated central square hole

This example has been studied by Kang and Lee in [15] using the non-dimensional dynamic influence function and more recently by Wu et al. in [16] using a differential quadrature method based on radial functions. The profile of the membrane is shown in Fig. 8, where the collocation points correspond to $N = 20$. As one can see, for this particular choice of N , the border of the inner square is sampled by the grid (the collocation points falling on the grid are rejected), and

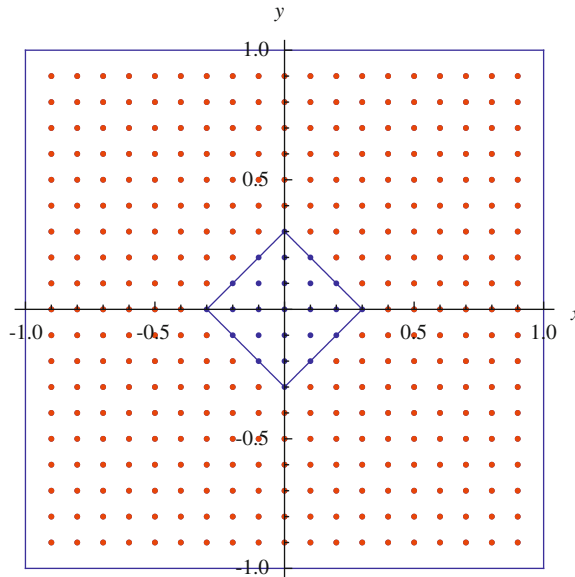


Fig. 8. Square membrane of side $\ell = 2$ with a square hole of side $\ell_0 = 3/5\sqrt{2}$, rotated by $\pi/2$ with respect to the outer square. The points in the figure correspond to a grid with $N = 20$.

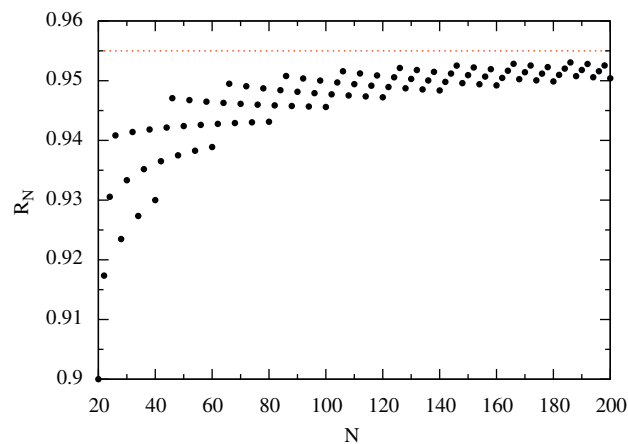


Fig. 9. Ratio of allowed to total points of the grid for a square membrane of side $\ell = 2$ with a square hole of side $\ell_0 = 3/5\sqrt{2}$, rotated by $\pi/2$ with respect to the outer square. The horizontal line is the geometric ratio.

therefore we may expect that the results obtained in this case are optimal. This situation repeats at N integer multiple of 20: this behavior is reflected in the plot of Fig. 9, where the ratio has local minima in correspondence to these points. It is easy to convince that if we had kept the collocation points falling on the internal border the ratio would have local maxima. A similar situation was discussed in [7] for the L-shaped membrane: in that case it was found that the two cases provide two monotonous sequences of approximation converging to the exact result from above and below, respectively. By performing a fit of the results corresponding to different grid sizes it was possible to obtain correctly the first 11 digits of the fundamental eigenvalue of the L-shape membrane.

Armed with this knowledge we have considered the same two sets for the present membrane, calling Set I (Set II) the set obtained after rejecting (keeping) the collocation points falling on the inner border. Taking advantage of the symmetry of the problem we have limited our study to the even-even modes of the membrane and we have obtained numerical approximations for the first five even-even frequencies for grids with N going from 20 to 200 and multiples of 20. In the case of the fundamental mode the calculation has been carried out up to grids with $N = 360$ (see Fig. 10). Since the two sets provide monotonous sequences of values converging to the exact results, at a fixed N they also provide a rigorous bound on the frequency itself. For example, for $N = 360$, we have the relation $3.624 < k_0 < 3.645$, which excludes all the values reported in [15,16] (actually, already for $N = 60$ all these values are excluded, as one can see from the figure).

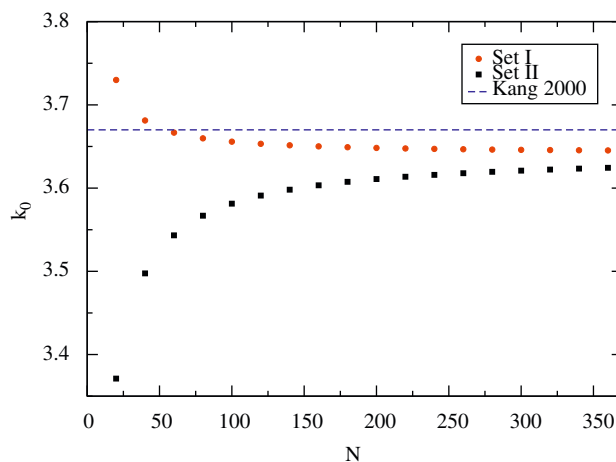


Fig. 10. Fundamental frequency for the square membrane of side $\ell = 2$ with a square hole of side $\ell_0 = 3/5\sqrt{2}$, rotated by $\pi/2$ with respect to the outer square. Set I (Set II) corresponds to rejecting (accepting) the points falling on the internal border. The horizontal line is the result of [15].

Table 7

First five even–even frequencies of the square membrane of side $\ell = 2$ with a square hole of side $\ell_0 = 3/5\sqrt{2}$, rotated by $\pi/2$ with respect to the outer square.

	$LSF_{220}^{(I)}$	$LSF_{220}^{(II)}$	$LSF_{FIT}^{(I)}$	$LSF_{FIT}^{(II)}$	LSF_{mixed}
k_0	3.6477	3.6136	3.64186	3.64186	3.6412
k_1	5.1718	5.1522	5.16786	5.16786	5.1672
k_2	6.4135	6.3897	6.40929	6.40929	6.4088
k_3	7.7117	7.6803	7.70717	7.70717	7.7069
k_4	8.5540	8.5199	8.54732	8.54732	8.5464

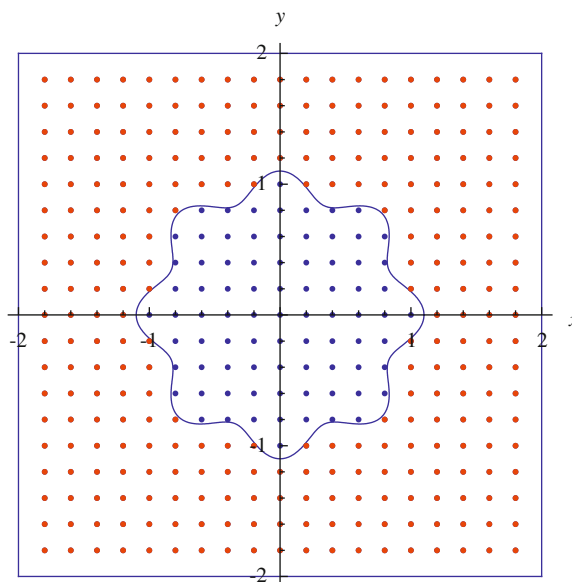


Fig. 11. Square membrane with a central hole described by the equation $r = 1 + \frac{1}{10}\sin[8(\phi + \pi/16)]$. The points in the figure correspond to a grid with $N = 20$.

In Table 7 we report the results obtained for the first five even–even frequencies of this membrane using our method. The second and third columns contain the values obtained by using Sets I and II with $N = 220$, which as mentioned above provide a rigorous bound on each frequency. The fourth and fifth columns contain the values obtained by fitting the

numerical results for the two sets of grids going from $N = 20$ up to $N = 220$ (with step $\Delta N = 20$) with the functional form

$$k^{\text{FIT}}(N) = c_0 + \sum_{k=1}^6 \frac{c_k}{N^k} + \frac{c_7}{N \log N},$$

remarkably the results agree to all digits shown. Finally the last column contains the results obtained by generating a new set which interpolated the two original sets, i.e. $k^{\text{mixed}}(N) = ak_{\text{I}}(N) + (1 - a)k_{\text{II}}(N)$. The parameter a is determined by requiring that the last two values of the sequence be equal. Although this estimate is less precise than the previous two it provides an independent check.

3.6. Example 6: square membrane with a central hole of complex shape

Our last application in two dimensions is to a square membrane with a central hole described by the equation

$$r = 1 + \frac{1}{10} \sin \left[8 \left(\phi + \frac{\pi}{16} \right) \right],$$

see Fig. 11. We have calculated the frequency of the fundamental mode of this membrane using LSF with N ranging from $N = 20$ to 220. We show the results in Fig. 12, where we also display the fit $k_0 = 2.64 - 1.9/N$. In Fig. 13 we display the frequency of the fundamental mode of this drum, obtained by fitting the numerical results in Fig. 12 from $N = 20$ to N^{max} and varying N^{max} . One can appreciate that the fitted value of k_0 is converging quite rapidly to a constant value.

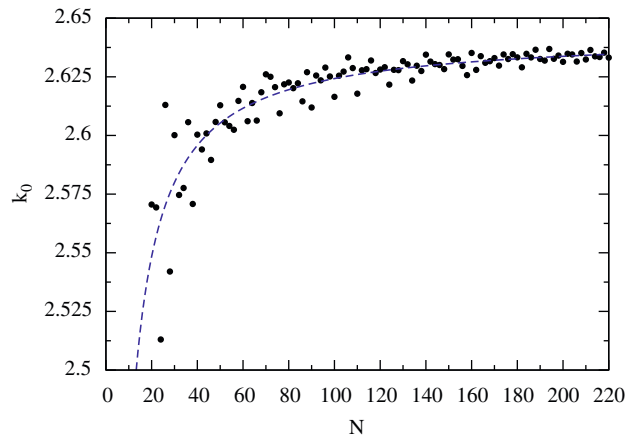


Fig. 12. Frequency of the fundamental mode of the drum with a central hole described by the equation $r = 1 + \frac{1}{10} \sin[8(\phi + \pi/16)]$ as a function of N . The dashed curve is the fit $k_0 = 2.64 - 1.9/N$.

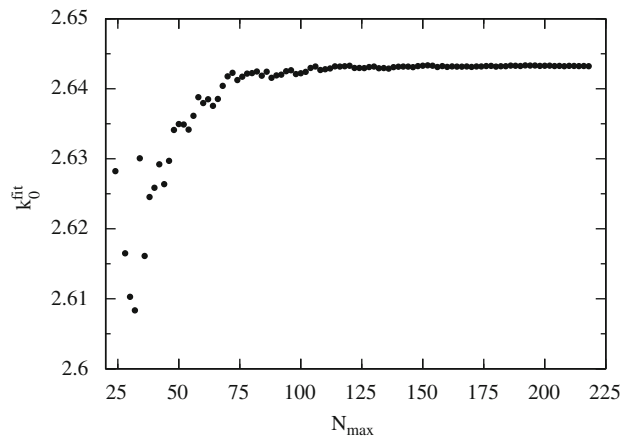


Fig. 13. Frequency of the fundamental mode of the drum of Fig. 12 obtained by fitting the numerical results in the figure from $N = 20$ to N^{max} and varying N^{max} .

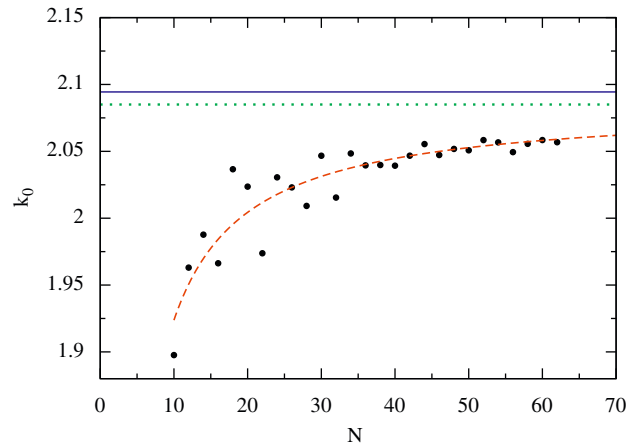


Fig. 14. Frequency of the fundamental mode of a spherical volume of radius $R = 2$ with an interior spherical hole of radius $r = \frac{1}{2}$ centered at the origin. The continuous horizontal line is the exact value $k_0^{\text{exact}} = 2.0944$, while the dashed curve corresponds to the fit: $k_0^{\text{fit}}(N) = 2.08501 - 1.61284/N$. The horizontal dotted line is the constant value $k_0 = 2.08501$ obtained from the fit for $N \rightarrow \infty$.

3.7. Example 7: spherical volume with a spherical hole

Although the main focus of the paper is on two-dimensional multiply connected membranes, we will discuss here a simple three-dimensional example, which is the direct generalization of our first example of the annular membrane. We consider a sphere of radius $R = 2$ with a spherical hole of radius $r = \frac{1}{2}$ at its center. Our method is applied along the lines explained in the last part of Section 2, the only difference with the previous examples being the dimensionality of the matrices obtained with the discretization. In particular, we have exploited the symmetry of the problem, which is invariant with respect to reflections about each coordinate axis, and used a set of LSF which are symmetrized in each direction. In this way the dimensionality of the matrix is reduced from $(N - 1)^3$ to $(N/2)^3$. Clearly the corresponding eigenvalues and eigenvectors only approximate the even–even–even part of the spectrum (the remaining parts may be obtained in a similar way). Using this approach we have been able to calculate the frequency of the fundamental mode for a large number of grid points, as shown in Fig. 14. The continuous horizontal line is the exact value, $k_0^{\text{exact}} = 2.0944$, while the dashed curve is the fit:

$$k_0^{\text{fit}}(N) = 2.08501 - 1.61284/N. \quad (17)$$

The green dotted line corresponds to the value $k_0 = 2.08501$ which is obtained from the fit for $N \rightarrow \infty$. This value is in quite good agreement with the exact result.

4. Conclusions

In this paper we have described a simple approach to the solution of the Helmholtz equation on multiply connected two-dimensional domains of arbitrary shape. We have compared the numerical results obtained by using this approach with those available in the literature for specific cases. We have found that a good precision could be achieved within our scheme, even with grids of modest size.

To be more explicit we may summarize the advantages of the present method in the following points:

- its generality; its application does not require a specific treatment of the different cases and all the procedure can be automatized from the start;
- the absence of spurious solutions;
- the possibility of using fine grids, since the matrices obtained by collocation are sparse the amount of memory needed in the calculation is reduced; the dimension of the matrices can be further reduced for problems which are symmetric with respect to the coordinate axes;
- the diagonalization of the matrix provides an approximation to a whole part of the spectrum of the membrane
- it can also deal with membrane with multiple holes;
- the extrapolation of the results corresponding to different grid sizes provide precise approximations for the eigenvalues, particularly for geometries where the border is sampled by the grid;
- the method can be applied also to inhomogeneous membranes (see [8]).

References

- [1] C.Y. Wang, On the polygonal membrane with a circular core, *Journal of Sound and Vibration* 215 (1998) 195–199.
- [2] J.T. Chen, J.H. Lin, S.R. Kuo, S.W. Chyuan, Boundary element analysis for the Helmholtz eigenvalue problems with a multiply connected domain, *Proceedings of the Royal Society A* 457 (2001) 2521–2546.
- [3] G. Chen, J. Zhou, *Boundary Element Methods*, Academic Press, Dordrecht, 1992.
- [4] J.T. Chen, L.W. Liu, H.K. Khong, Spurious and true eigensolutions of Helmholtz BIEs and BEMs for a multiply connected problem, *Proceedings of the Royal Society A* 459 (2003) 1891–1924.
- [5] J.T. Chen, I.L. Chen, Y.T. Lee, Eigensolutions of multiply connected membranes using the method of fundamental solutions, *Engineering Analysis with Boundary Elements* 29 (2005) 166–174.
- [6] S.Yu. Reutskiy, The method of fundamental solutions for Helmholtz eigenvalue problems in simply and multiply connected domains, *Engineering Analysis with Boundary Elements* 30 (2006) 150–159.
- [7] P. Amore, Solving the Helmholtz equation for membranes of arbitrary shape, *Journal of Physics A* 41 (2008) 265206.
- [8] P. Amore, A new method for studying the vibration of non-homogeneous membranes, *Journal of Sound and Vibration* 321 (2009) 104–114.
- [9] P. Amore, M. Cervantes, F.M. Fernández, Variational collocation on finite intervals, *Journal of Physics A* 40 (2007) 13047–13062.
- [10] P. Amore, Alternative representation of nonlocal operators and path integrals, *Physical Review A* 75 (2007) 032111.
- [11] D. Baye, Constant step Lagrange meshes for central potentials, *Journal of Physics B* 28 (1995) 4399–4412.
- [12] P. Amore, F.M. Fernández, R. Sáenz, K. Salvo, Collocation on uniform grids, *Journal of Physics A* 42 (2009) 115302.
- [13] J.R. Kuttler, V.G. Sigillito, Eigenvalues of the Laplacian in two dimensions, *SIAM Review* 26 (1984) 163–193.
- [14] J.T. Chen, L.W. Liu, S.W. Chyuan, Acoustic eigenanalysis for multiply connected problems using dual BEM, *Communications in Numerical Methods in Engineering* 20 (2004) 419–440.
- [15] S.W. Kang, J.M. Lee, Application of free vibration analysis of membranes using non-dimensional dynamic influence function, *Journal of Sound and Vibration* 234 (2000) 455–470.
- [16] W.X. Wu, C. Shu, C.M. Wang, Vibration analysis of arbitrarily shaped membranes using local radial basis function-based differential quadrature method, *Journal of Sound and Vibration* 306 (2007) 252–270.